Chemical Engineering Science 201 (2019) 167–174

Contents lists available at ScienceDirect

Chemical Engineering Science

journal homepage: www.elsevier.com/locate/ces

Self-healing anion exchange membrane for pH 7 redox flow batteries

Jianqiu Hou, Yahua Liu, Yazhi Liu, Liang Wu, Zhengjin Yang *, Tongwen Xu *

CAS Key Laboratory of Soft Matter Chemistry, Collaborative Innovation Center of Chemistry for Energy Materials, School of Chemistry and Material Science, University of Science and Technology of China, Hefei 230026, PR China

HIGHLIGHTS

- A self-healing AEM was prepared from styrene derivatives.
- Exploiting Diels-Alder reaction, the AEM can self-heal at 150 °C.
- The AEM can be applied in pH 7 aqueous organic redox flow battery.
- Coulombic efficiency maintains at 97% and energy efficiency exceeds 79%.

GRAPHICAL ABSTRACT

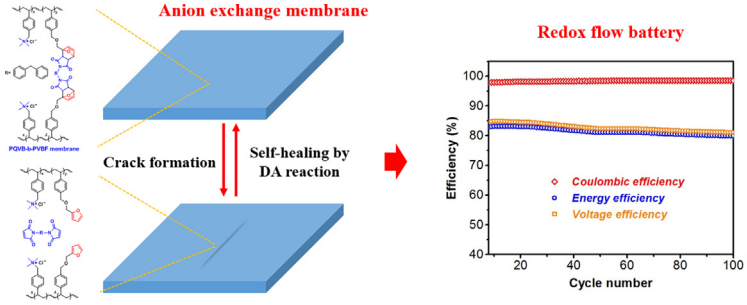

ARTICLE INFO

Article history:
Received 22 November 2018
Received in revised form 18 February 2019
Accepted 19 February 2019
Available online 6 March 2019

Keywords:
Anion exchange membrane
Self-healing
Diels-Alder reaction
Dynamic covalent bond
Organic aqueous redox flow battery

ABSTRACT

Anion exchange membranes (AEMs) separate the redox active electrolytes and transfer the charge carriers in redox flow batteries. During the long-term operation of a redox flow battery, the formation and propagation of cracks in AEMs are detrimental, resulting in capacity loss and self-discharge, while replacing the cracked membranes would increase the cost. Here we incorporate self-healing to an AEM through reversible and temperature-controlled Diels-Alder (DA) reaction. We first synthesized a block copolymer from vinylbenzyl chloride and 2-((4-vinylbenzyloxy) methyl) furan by RAFT polymerization. The benzylic chloride moiety was quaternized with trimethylamine to conduct anions, while bismaleimide was added to dynamically connect the furan moieties via DA reaction. By solution casting and reacting at 80 °C, an AEM with dynamic network was prepared. When evaluated for practical application, we found the AEM has a Cl^- conductivity of 32.7 mS cm^{-1} at 80 °C and man-made cracks on the membrane can be self-healed. We then tested its performance in a pH 7 aqueous organic redox flow battery, where it delivered stable cycling performances over 100 consecutive charge/discharge cycles, with a coulombic efficiency of >97% and an energy efficiency of >79%. This membrane is promising for practical applications and what we report here is a useful strategy in rendering conventional AEMs with self-healing property.

© 2019 Published by Elsevier Ltd.

1. Introduction

Anion exchange membranes (AEMs) have been widely used in energy conversion and energy storage devices, for instance, fuel cells and redox flow batteries (Ran et al., 2017). In these devices, AEMs conduct anions and in the meantime, separate the cathode reaction from the anode reaction (Zhang et al., 2015). The long-term stability of a fuel cell or a redox flow battery is of primary concern in practical application, which imposes a strict requirements on the mechanical stability of AEMs (He et al., 2016). The water swelling of AEM (caused by the high content of ion exchange groups in membrane) (Lin et al., 2017) and the build-up of pressure (from device-assembly and fluid) inside the cell stack (Mehmood et al., 2015) could potentially lead to the formation and propagation of cracks (Chen et al., 2002). These cracks can hardly be repaired due to the fact that most AEMs are cross-linked by

* Corresponding authors.
E-mail addresses: yangzj09@ustc.edu.cn (Z. Yang), twxu@ustc.edu.cn (T. Xu).

https://doi.org/10.1016/j.ces.2019.02.033
0009-2509/© 2019 Published by Elsevier Ltd.

covalent bonds (Taylor and In Het Panhuis, 2016) and the movement of polymer chains was impeded. Even micro-cracks will result in the obvious leakage of electrolyte, thereby causing capacity fade of the battery. To ensure the stable performance of a battery system, these AEMs must be replaced with new ones, which is not cost-effective and the disposed AEM materials could not be reprocessed (Sumerlin, 2018).

To address the challenge, here we report a tailor-made AEM with self-healing property. Self-healing is a fascinating property in living creatures (Tang and Marshall, 2017). For example, our skin can repair from damage thus restore functions. This striking feature inspired researchers to synthesize self-healing polymers (Trovatti et al., 2015). The self-healing inside a synthetic polymer is based on reversible chemical bonds (Cao et al., 2017). Once the wounds were formed, new chemical bonds were formed nearby the wounds and the damage was then repaired (Lai et al., 2016). These reversible chemical bonds could originate from hydrogen bonds (Tee et al., 2012), schiff-base reaction (Li et al., 2016), boroxines (Röttger et al., 2017) and Diels-Alder (DA) reaction (Fuhrmann et al., 2016). While most of them are utilized to fabricate hydrogels (Wang et al., 2018) and elastomers (Wu et al., 2017), the exploit of self-healing is rarely reported in energy-related devices. Very recently, a proton exchange membrane for fuel cell with self-healing property was reported (Li et al., 2018). The hydrogen bond, they used, can reversibly combine Nafion and polyvinyl alcohol, leading to membrane self-heal. However, there is no report on self-healing AEMs, especially those based on dynamic covalent bonds and cross-linked to suppress membrane swelling.

As a proof of concept, we targeted at AEMs that work in aqueous solution and reported here a self-healing AEM based on aqueous-stable and temperature-controlled DA reaction between furan and maleimide groups (Zhang et al., 2016). We first attached furan groups to vinylbenzyl chloride (VBC) via Williamson reaction (Kuhl et al., 2012). Through reversible addition fragmentation transfer (RAFT) polymerization, we synthesized a block copolymer containing poly(vinylbenzyl chloride) and poly(2-((4-vinylbenzyloxy)methyl)furan) segments. The benzylic chloride moiety was quaternized with trimethylamine to conduct anions, while bismaleimide was introduced during solution casting to dynamically connect the furan moieties by exploiting the reversible DA reaction between them. We successfully obtained an AEM that has a Cl^- conductivity of 32.7 mS cm^{-1} at 80 °C and self-healing capability. We then tested its performance in a pH 7 aqueous organic redox flow battery, where it delivered stable cycling performance over 100 consecutive charge/discharge cycles, with a coulombic efficiency of >97% and an energy efficiency of >79%. Our results demonstrate that this strategy is promising in rendering conventional AEMs with self-healing property.

2. Experimental

2.1. Materials

4-vinylbenzyl chloride (VBC) was purified on alkaline aluminum oxide column. Dimethyl sulfoxide (DMSO), furfuryl alcohol, anhydrous sodium sulfate, ethyl acetate, hexane, toluene, methanol, chloroform, 1-methyl-2-pyrrolidinone (NMP), dimethyl formamide (DMF), styrene, divinylbenzene, disodium chloride, sodium bicarbonate, and trimethylamine alcoholic solution (33 wt%) were purchased from Sinopharm Chemical Reagent Co., Ltd. (Shanghai, P.R. China). 2-cyano-2-propyl dodecyl trithiocarbonate, 2, 2-azobisisobutyronitrile (AIBN), 4,4′-dimaleimidophenyl methane and 4-hydroxy-2,2,6,6-tetramethylpiperidin-1-oxyl (4-OH-TEMPO) were purchased from Energy Chemicals (Shanghai, P. R. China). AIBN was recrystallized in alcohol. Bis(3-trimethylammonio)propyl viologen tetrachloride (BTMAP-Vi) was synthesized according to a reported procedure (Beh et al., 2017). ^{1}H NMR (400 MHZ, D_2O): δ 9.24 (d, 4H), 8.66 (d, 4H), 4.90 (t, 4H), 3.63 (m, 4H), 3.24 (s, 18H), 2.73 (m, 4H).

2.2. 2-((4-vinylbenzyloxy) methyl) furan

Furfuryl alcohol (1.9 g, 19.5 mmol) and sodium hydroxide (1.6 g, 40.0 mmol) were added to DMSO (12 mL), stirred at room temperature for 20 min and then 4-vinylbenzyl chloride (4.2 g, 27.5 mmol) was added. After stirring at 45 °C for 12 h, water (50 mL) was added. The mixture was then extracted with ethyl acetate (3 × 30 mL), and the combined organic layer was dried over anhydrous sodium sulfate, filtered and concentrated on a rotary evaporator. Column chromatography on silica gel (ethyl acetate: hexane = 1:50) afforded the product as colorless oil (2.4 g, 58%), referred to as VBF. ^{1}H NMR (400 MHz, $CDCl_3$), δ (ppm): 7.41 (dd, 1H, CH), 7.40–7.29 (m, 4H, CH), 6.67–6.74 (m, 1H, CH), 6.34 (dd, 1H, CH), 6.32 (d, 1H, CH), 5.76–5.71 (dd, H, CH), 5.24–5.21 (dd, H, CH), 4.52 (s, 2H, CH_2), 4.46 (s, 2H, CH_2).

2.3. Poly(4-vinlybenzyl chloride)

4-vinylbenzyl chloride (VBC) (2.5 g, 16.3 mmol), AIBN (0.001 g, 0.006 mmol), 2-cyano-2-propyl dodecyl trithiocarbonate (0.03 g, 0.087 mmol) and toluene (2.5 mL) were added to a flask. The mixture was subjected to three freeze-pumpthaw cycles and then heated to 60 °C for 72 h *in vacuo*. Upon completion, the mixture was precipitated in methanol (50 mL) and filtered. The filter cake was dissolved in chloroform (10 mL), precipitated from methanol (100 mL), filtered and dried *in vacuo* to obtain the pure product, Poly(4-vinlybenzyl chloride) (PVBC) the molecular weight of which was characterized by gel permeation chromatography (Mn = 13,500 g mol^{-1}, Mw = 15,200 g mol^{-1}, PDI = 1.12).

2.4. Poly(4-vinlybenzyl chloride)-b-poly(2-((4-vinylbenzyloxy) methyl)furan)

2-((4-vinylbenzyloxy)methyl)furan (VBF, 1.54 g, 7.2 mmol), PVBC (0.96 g, 0.071 mmol), AIBN (0.001 g, 0.006 mmol) and toluene (2.5 mL) were added to a flask. The mixture was subjected to three freeze-pumpthaw cycles and then heated to 60 °C for 168 h. The mixture was precipitated in methanol (50 mL) and filtered. The filter cake was dissolved in chloroform (10 mL), precipitated from methanol (100 mL), filtered and dried *in vacuo* to obtain pure product, referred to as PVBC-b-PVBF. The ratio of PVBF segments to PVBC segments calculated from ^{1}H NMR is 1:0.88. The molecular weight was characterized by gel permeation chromatography (Mn = 22,200 g mol^{-1}, Mw = 39,000 g mol^{-1}, PDI = 1.76).

2.5. Anion exchange membrane preparation

PVBC-b-PVBF was dissolved in 1-methyl-2-pyrrolidinone (5 wt %) and slightly excess trimethylamine (alcoholic solution, 30 wt%) was added to the polymer solution. The mixture was stirred at room temperature for 8 h and 4,4′-dimaleimidophenylmethane (0.5 equiv to the furan groups in polymer) was then added. The solution was stirred at room temperature for another 2 h. The resulting solution was cast on a clean glass plate and heated at 80° C to evaporate all the solvent. A free standing membrane cross-linked via DA reaction, PQVB-b-PVBF, was obtained and peeled off. Counter ion exchange was conducted by immersing the membrane samples in NaCl (1 mol L^{-1}), Na_2SO_4 (0.5 mol L^{-1}) or $NaHCO_3$ (1 mol L^{-1}) aqueous solution.

2.6. Characterization methods

2.6.1. Nuclear magnetic resonance

^{1}H NMR spectra were conducted on a Bruker Avance III 400 MHz spectrometer, using $CDCl_3$ as solvent.

2.6.2. Gel permeation chromatography

Molecular weight (M_n, M_w) and polymer dispersity index (PDI = M_w/M_n) of the polymers was investigated by gel permeation chromatography (GPC) using a PL 120 Plus (Agilent Technologies co., Ltd, China) equipped with differential refractive index detector. Three PL Gel Mixed Carbon 18 SEC columns connected in series were used. Samples were freshly prepared in THF (HPLC grade) and THF (HPLC grade) was used as the eluent at a flow rate of 1.0 mL min^{-1}. The detection system was calibrated with a polystyrene reference sample (M_w = 110 K) of 2 mg mL^{-1}.

2.6.3. Ion exchange capacity (IEC)

IEC of the membrane samples was measured by the Mohr's method. Membrane samples in Cl^- form were immersed in aqueous Na_2SO_4 solution (0.5 mol L^{-1}) for 8 h. After removing the membrane samples, Cl^- content in the solution was titrated with aqueous $AgNO_3$ solution (0.01 mol L^{-1}) and K_2CrO_4 was used as the indicator. The *IEC* values were calculated by Eq. (1):

$$\mathrm{IEC} = \frac{V \times C}{W_{dry}} \tag{1}$$

where V is the consumed volume of $AgNO_3$ in titration, C is the concentration of aqueous $AgNO_3$ solution (0.01 mol L^{-1}) and W_{dry} is the weight of dry membrane sample in Cl^- form.

2.6.4. Conductivity measurement

Ion conductivity of membrane samples was measured by the four-point probe technique (on a Zahner Zemmiun E workstation) with potentiostatic mode (amplitude 50 mV, frequency range 1 MHz-100 Hz). The membrane sample (1 cm × 4 cm, Cl^-, SO_4^{2-} or HCO_3^- form) was placed in a Teflon cell which has two current collecting electrodes and two potential sensing electrodes (the distance between couple electrodes is 1 cm). The membrane sample was completely immersed in deionized water. The ionic conductivity was calculated by Eq. (2):

$$\sigma = \frac{\mathrm{L}}{RWd} \tag{2}$$

where R is the membrane resistance, L is the distance between potential sensing electrodes. W and d are the width (here 1 cm) and thickness of the membrane, respectively. Before each measurement, the samples were equilibrated for at least 30 min.

2.6.5. Water uptake and swelling ratio

Membrane samples (1 cm × 4 cm, in OH^- form) were immersed in deionized water for 24 h. They were then taken out and water on the surface was quickly wiped with tissue paper. The weight and length of wet membrane samples were recorded. After drying the membrane samples at 60 °C for 24 h, the weight and length of dry membrane samples were also recorded. Water uptake (WU) was calculated by Eq. (3):

$$WU = \frac{W_{wet} - W_{dry}}{W_{dry}} \times 100\% \tag{3}$$

where W_{wet} is the weight of wet membrane sample and W_{dry} is the weight of dry membrane sample.. Swelling ratio (SR) of the membrane samples was characterized by linear expansion ratio, which was calculated by eq.4:

$$SR = \frac{L_{wet} - L_{dry}}{L_{dry}} \times 100\% \tag{4}$$

where L_{wet} is the length of wet membrane sample and L_{dry} is the length of dry membrane sample.

2.6.6. Thermal and mechanical property

Thermal stabilities of the membrane and polymer samples were measured on a Q5000 thermo-gravimetric analyzer (TA Instruments, USA) under N_2 atmosphere and at a heating rate of 10 °C min^{-1} from room temperature to 650 °C.

Differential scanning calorimetry was carried out on a Q2000 Differential Scanning Calorimetry (TA instrument, USA). The sample was first heated from 30 °C to 160 °C followed by cooling to 30 °C then re-heated to 160 °C at a heating/cooling rate of 10 °C min^{-1} under N_2 atmosphere.

Tensile strength measurements of hydrated membrane samples were performed on a Q800 dynamic mechanical analyzer (TA Instruments, USA) at a stretching rate of 0.5 N min^{-1}.

2.6.7. Membrane self-healing

To monitor the self-healing of the as-prepared AEM samples, a crack was made on the surface of a membrane sample. The injured membrane was observed by a TM3000 scanning electron micrograph (SEM, HITACH, Japan). We then clamped it with two polytetrafluoroethylene plates and heated at 150 °C for 1 h. After slowly cooling to room temperature, the same membrane sample was observed again by SEM.

2.6.8. Flow battery test

The positive electrolyte was prepared by dissolving 4-hydroxy-2,2,6,6-tetramethylpiperidin-1-oxyl (4-OH-TEMPO, 0.17 g) in 1 M NaCl solution (10 mL) and the negative electrolyte was prepared by dissolving bis(3-trimethylammonio)propyl viologen tetrachloride (BTMAP-Vi, 0.5 g) in 1 M NaCl solution (10 mL). Cell hardware was purchased from Fuel Cell Tech (Albuquerque, USA). Pyrosealed POCO graphite flow plates with serpentine flow fields were used on both sides. The electrode comprised 3 stacked sheets of Sigracet SGL 39AA carbon paper, with an effective area of 5 cm^2. A piece of PQVB-b-PVBC membrane (thickness: 188 μm), with the effective area of 5 cm^2, was sandwiched between the positive and the negative electrodes. The rest of the space between the plates was sealed by Viton gaskets. The electrolytes were pumped into the cell stack using Masterflex L/S peristaltic pump (Cole-Parmer, Vernon Hills, IL) at a pumping rate of 60 rpm. Polarization curves were obtained by charging the cell to certain states of charge (SOC), then polarized by linear sweep voltammetry on a Bio-Logic BCS-815. Galvanostatic cell cycling was performed at the current density of 10 mA cm^{-2} with cutoff voltages at 1.6 V for the charge process and 0.5 V for the discharge process.

3. Results and discussion

3.1. Self-healing AEM preparation

An AEM is normally composed of a polymer backbone, to which positively charged functional groups are attached. The synthesis of an AEM could therefore start from polymerizing monomers or by the post-functionalization of existing polymers. We chose the former method here because it enables us to precisely tune the amount of functional groups and to easily introduce functionalities that lead to membrane self-healing. The monomers we selected here are styrene derivatives due to their high reactivity in polymerization reaction.

The first monomer we used is 4-vinylbenzyl chloride (VBC), which is commercially available and has benzylic chloride moieties that can later on be converted into quaternary ammonium functional groups, ion exchange functionalities of an AEM.

The second monomer is a VBC derivative, VBF, to which furan groups were attached via a facile one-step Williamson reaction, as shown in Fig. 1a. Structure of VBF was confirmed by ^{1}H NMR. The single peaks at 4.52 ppm (H6) and 4.46 ppm (H7) belong to the methylene protons between the benzene ring and the furan ring. The rest of the protons on furan ring was observed at 7.41, 6.71, 6.34 and 6.32 ppm, respectively (Fig. 2a). The peaks we observed matched exactly the structure of VBF.

VBC and VBF were then polymerized by reversible addition fragmentation transfer (RAFT) polymerization (An et al., 2005), which could give well-controlled molecular weight distribution thereby ensuring reproducible membrane properties. Through a successive two-step RAFT polymerization as shown in Fig. 1a, the first segment, the poly(vinylbenzyl chloride) segment, has a molecular weight of Mn = 13,500 g mol^{-1}, (Mw = 15,200 g mol^{-1}, PDI = 1.12) and its ^{1}H NMR spectrum is shown in Fig. 2b. The second segment, which was block-copolymerized onto the poly(vinylbenzyl chloride) segment, contains furan moieties, as confirmed by the ^{1}H NMR peak at 7.4 ppm (Fig. 2c). Finally, a block copolymer, poly(vinylbenzyl chloride)-b-poly(vinylbenzyl furan) (PVBC-b-PVBF) was obtained, with a molecular weight of Mn = 22,200 g mol^{-1}, (Mw = 39,000 g mol^{-1}, PDI = 1.76). The ^{1}H NMR peak at 4.4 ppm belongs to the methylene protons between the benzene ring and the furan ring (Fig. 2c). By calculating the integration ratio of peak at 7.4 ppm to the peak at 4.4 ppm, the molar content of PVBC segment and PVBF segment is 46% and 54%, respectively, close to the molar feed ratio of VBC to VBF (1:1).

To make a membrane, the PVBC-b-PVBF was dissolved in NMP and the benzylic chloride moieties on the PVBC segment were quaternized at room temperature with excess amount of trimethylamine in solution, leading to quaternary ammonium functional groups that can conduct anions. Then, bismaleimide was added, which can react with the furan ring on the PVBF segment through reversible Diels-Alder reaction at elevated temperature (Fig. 1b). The resulting homogeneous solution, as shown in Fig. 3a, was poured into a super flat petri-dish. Finally, evaporating the solvent at 80 °C and initializing the reversible DA reaction afforded a transparent, brownish free-standing AEM, namely, PQVB-b-PVBF, as shown in Fig. 3b.

The PQVB-b-PVBF membrane we obtained, as we have designed, has a cross-linked network. Therefore, when we immersed the membrane samples in DMF, the samples cannot be dissolved, while slightly swell (Fig. 3c). The crosslinking in the membrane matrix is dynamic as we have anticipated. As we heated the mixture at 150 °C for 1 h, the membrane samples dissolve and form a homogenous solution due to the cleavage of dynamic bonds

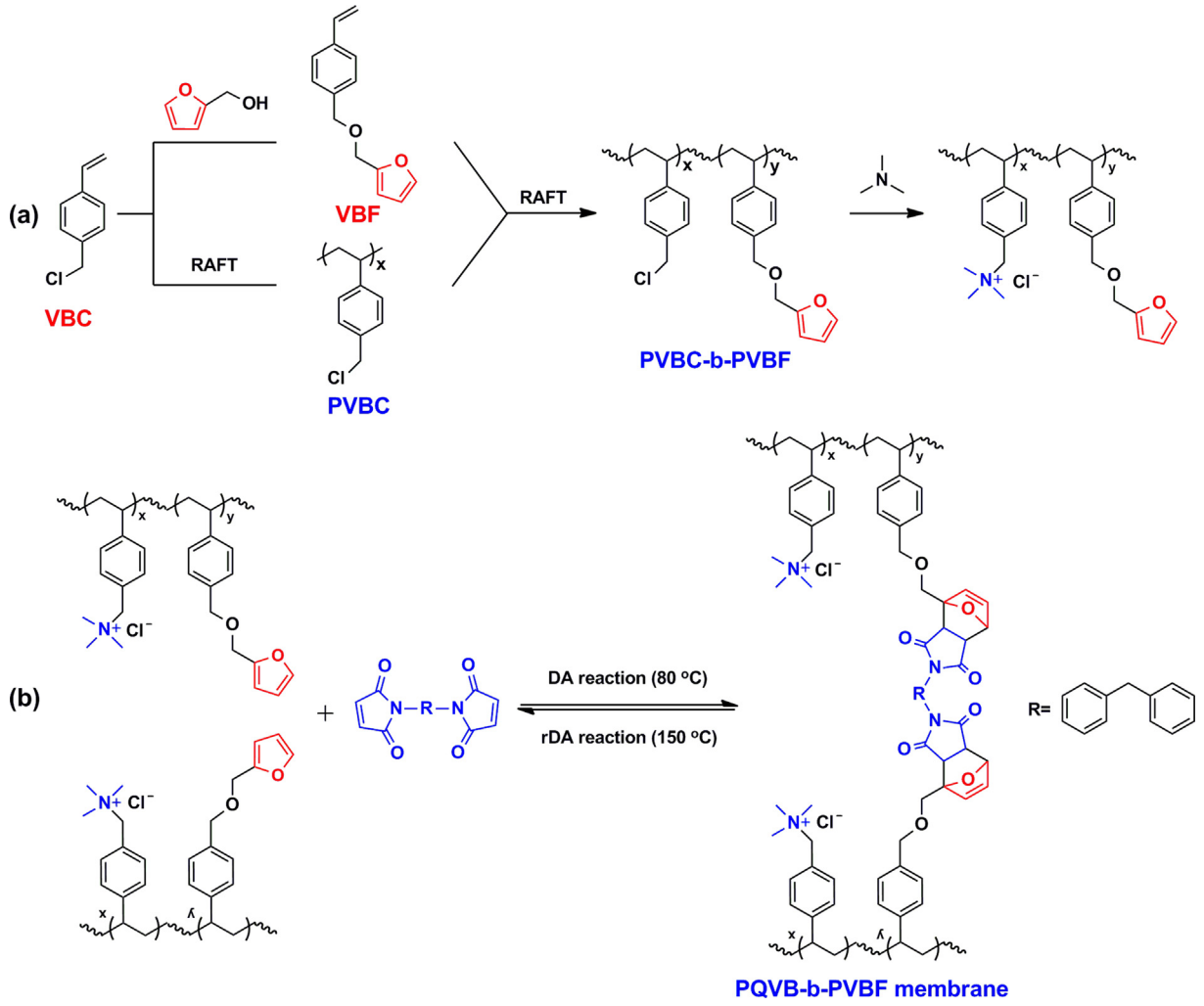

Fig. 1. The synthesis of a self-healing AEM from 4-vinylbenzyl chloride (VBC) and its derivatives. (a) 2-((4-vinylbenzyloxy) methyl) furan (VBF) was synthesized via a Williamson reaction between VBC and furfuryl alcohol; PVBC was synthesized by RAFT polymerization. Copolymerizing VBF and PVBC oligomer yielded PVBC-b-PVBF, which was further quaternized by a Menshutkin reaction with trimethylamine. (b) The AEM self-healing mechanism. The as-prepared AEM material, PQVB-b-PVBF, can react with bismaleimde at 80 °C to form dynamic covalent bonds based on reversible Diels-Alder reaction. The bonds can be broken at 150 °C when retro Diels-Alder reaction occurs.

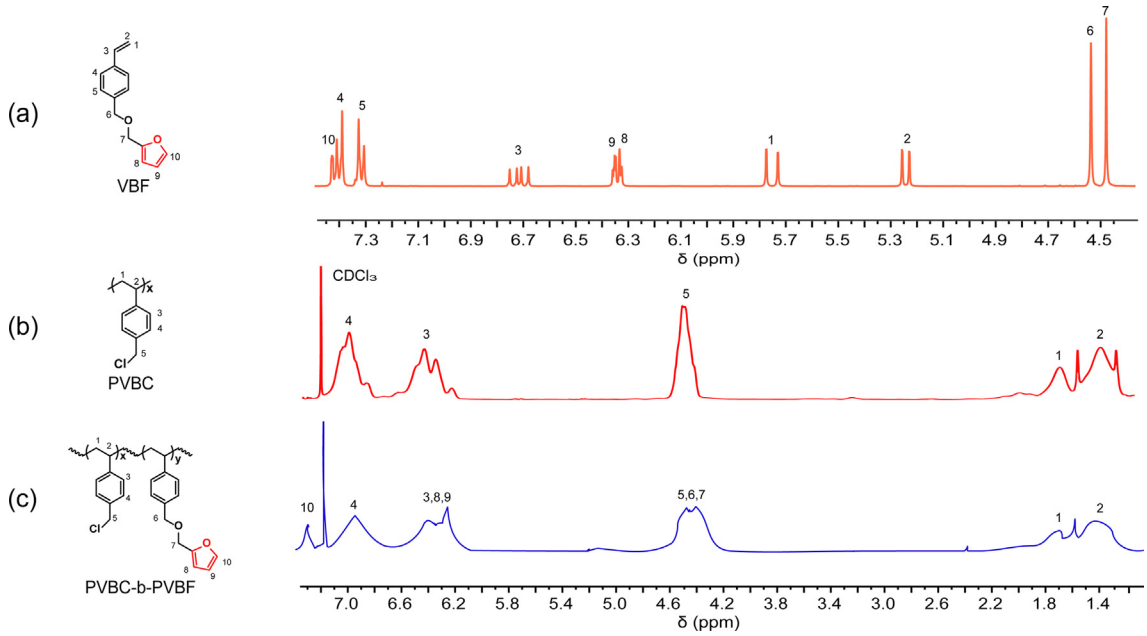

Fig. 2. The ^{1}H NMR spectrum of (a) 2-((4-vinylbenzyloxy) methyl) furan (VBF), (b) poly(4-vinlybenzyl chloride), PVBC, and (c) PVBC-b-PVBF. $CDCl_3$ is used as solvent.

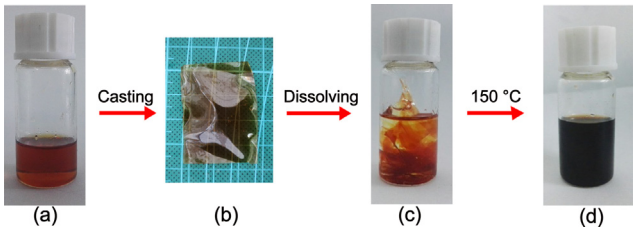

Fig. 3. Images demonstrate that casting (a) a PQVB-b-PVBF solution on a clean glass plate afforded (b) a robust and free-standing AEM. (c) The membrane did not dissolve in DMF at room temperature or at 80 °C, the temperature at which the solvent was evaporated. (d) Heating the mixture to 150 °C at which the retro Diels-Alder reaction occurs, a homogeneous solution was formed.

(Fig. 3d), implying that the retro DA (rDA) reaction occurs. Noting that the color of the solution becomes darker due to the radical polymerization of bismaleimide at high temperature (Haas and MacDonald, 1973). This is proved by heating a solution of bismaleimide in DMF (1 wt%) at 150 °C for 1 h, which also turns dark. As a control, we prepared another cross-linked membrane from styrene and divinylbenzene (DVB), and the structure is shown in Supporting Fig. S1a. When we treated the membrane in DMF at 150 °C for 1 h, the membrane cannot be dissolved and can only be swelled (Supporting Fig. S1b and Fig. S1c). The results indicate that 150 °C is an appropriate temperature for membranes to self-heal because the bonds from DA reaction inside the membrane matrix will break and form in a dynamic equilibrium at 150 °C.

3.2. Membrane conductivity and water swelling

Cl^- conductivity of the PQVB-b-PVBF membrane, with an ion exchange capacity (IEC) of 1.69 mmol g^{-1}, was measured in water at temperatures ranging from 30 °C to 80 °C. The Cl^- conductivity of PQVB-b-PVBF membrane at 30 °C is 9.5 mS cm^{-1}, which is increased to 32.7 mS cm^{-1} at 80 °C (Fig. 4). HCO_3^- and SO_4^{2-} conductivity of PQVB-b-PVBF membrane were also measured. As the temperature increases from 30 °C to 80 °C, the HCO_3^- conductivity increases from 5.6 mS cm^{-1} to 14.9 mS cm^{-1} and we also observed an increase of SO_4^{2-} conductivity from 14.3 mS cm^{-1} to

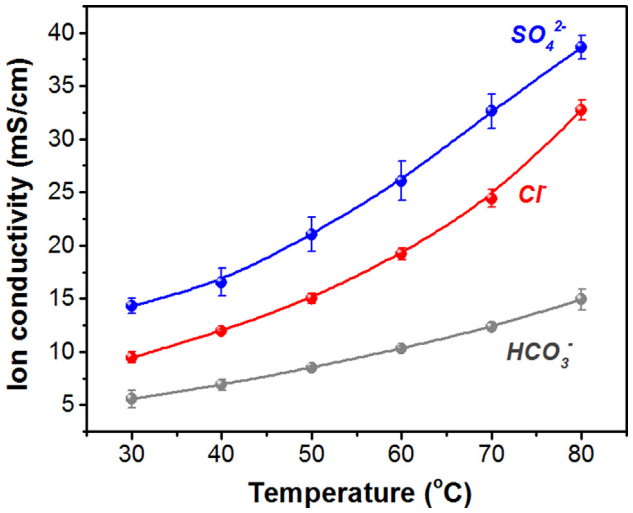

Fig. 4. SO_4^{2-}, Cl^- and HCO_3^- conductivity of PQVB-b-PVBF membrane as functions of operating temperature.

38.6 mS cm^{-1}. The different conductivities of Cl^-, HCO_3^- and SO_4^{2-} ions can be ascribed to the difference in the size of hydrated ions and hydrophobicity. For example, Cl^-, with smaller hydrated radius, move through the membrane faster than larger hydrated ions, such as HCO_3^- (Amel et al., 2016). Besides, Cl^- is more hydrophobic due to its low hydration, resulting in the slower transfer across the hydrophilic AEM, as compared to SO_4^{2-} (Sata et al., 1995).

We compared the conductivity of PQVB-b-PVBF to other reported AEMs, as in Table 1 and we found that PQVB-b-PVBF has superior conductivity than most AEMs. This promises its potential application in a fuel cell or a redox flow battery application, which will be demonstrated in a later section.

For practical applications, water swelling and anion conductivity are both vital. The PQVB-b-PVBF membrane in Cl^- from has a water uptake of 46.6% and swelling ratio of 16.0% at 30 °C. The moderate amount of water uptake benefits the conduction of

Table 1
Ion exchange capacity (IEC), water uptake (WU), swelling ratio (SR) and Cl^- conductivity of PQVB-b-PVBC at 30 °C, compared with those of reported membranes at 30 °C or room temperature.

Membrane	IEC (mmol g^{-1})	WU (%)	SR (%)	Cl^- conductivity (mS cm^{-1})	Reference
PQVB-b-PVBF	1.69	46.6	16.0	9.5	This work
RC-QPPO-1.78	1.78	41.3	15.4	11.4	Hou et al. (2018)
VPPO/VBC-IPN	1.83	2.30	0.97	12.0	Yang et al. (2015)
$PVBC_{100}$-b-$PBeS_{183}$	2.00	45	–	11.6	Wang and Hickner (2014)
X60Y30C16	1.80	18	13.2	4.9	Zhu et al. (2016)
X60Y60	1.83	15	10.6	4.2	Zhu et al. (2016)
X60Y30C6	2.06	22	15.2	6.7	Zhu et al. (2016)
X60Y30C10	2.03	21	14.5	5.4	Zhu et al. (2016)
$^{0.55}Ni_{PEO}$	1.26	193	–	6	Kwasny et al. (2018)

anions across the membrane matrix, while the membrane swelling was suppressed by the Diels-Alder bond crosslinking. When compared with other AEMs with cross-linked polymer network (Table 1), PQVB-b-PVBF has superior conductivity than most of other cross-linked AEMs and we conclude that the dynamic Diels-Alder crosslinking can provide the same function as other permanent crosslinking methods.

3.3. Thermal property

Thermal gravimetric analysis (TGA) curve of PQVB-b-PVBF membrane reveals three distinct weight-loss peak (Fig. 5). A small amount of weight loss occurred at 71 °C, which is associated with the evaporation of adsorbed water. A second weight loss peak was observed at 262 °C, corresponding to the degradation of quaternary ammonium functional groups. Finally, at 432 °C, the polymer backbone degradation happens. These results indicate that the PQVB-b-PVBF membrane is stable enough at 150 °C, the temperature we used to observe the self-healing properties of the membrane samples. It is worth noting that no polymer melting is observed at temperature up to 150 °C.

Differential Scanning Calorimeter (DSC) curve was measured to evaluate whether the polymer is flexible enough at the self-healing temperature (150 °C). The glass transition temperature (Tg) of PVBC-b-PVBF is 86 °C (Supporting Fig. S2), much lower than the self-healing temperature. Thus, when we heated the membrane samples to the self-healing temperature, the polymer chains will be in the elastomeric state and flexible.

3.4. Self-healing property

The reversible and thermally responsive Diels-Alder reaction were embedded in the PQVB-b-PVBF membrane matrix. When the membrane is cracked, new bonds will be formed around the crack as long as temperature is high enough to initiate rDA reaction, thereby the membrane is self-healed. The self-healing test of PQVB-PVBF membrane was conducted according to reported procedure (Jo et al., 2017; Kavitha and Singha, 2009), as shown in Fig. 6a. At first, we made a crack on the membrane surface with a sharp knife. The cracked membrane sample was fixed on a metal plate and scanning electron microscopy image was recorded (SEM, Fig. 6b). We then sandwiched the membrane sample with two polytetrafluoroethylene plates and heated the sample to 150 °C. During heat treatment, the bonds formed by DA reaction break and form in a dynamic equilibrium. One hour later, SEM image shows that crack disappears (Fig. 6b). The disappearance of crack in the PQVB-b-PVBF membrane sample was not caused by polymer melting, because as we have proved the temperature is not high enough to melt the polymer. In a control experiment, we conducted the same procedure on a divinyl benzene (DVB) cross-linked polystyrene (PS) membrane and we found the crack still existed even after long-time thermal treatment. Even when high pressure was applied, the crack still exists, although the width of the crack might be narrowed (Fig. 6c). Our results confirmed that the PQVB-b-PVBF membrane sample has the capability of healing cracks.

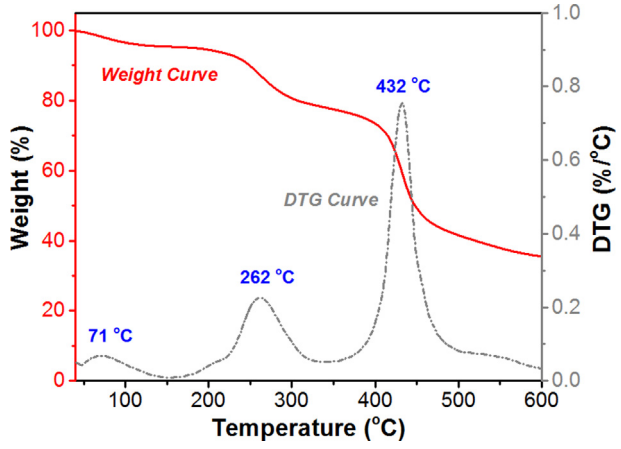

Fig. 5. TGA and DTG curves of PQVB-b-PVBF membrane. A two-step weight loss starting around 262 °C and 432 °C is observed. The tiny amount of weight loss at 71 °C is caused by the evaporation of adsorbed water.

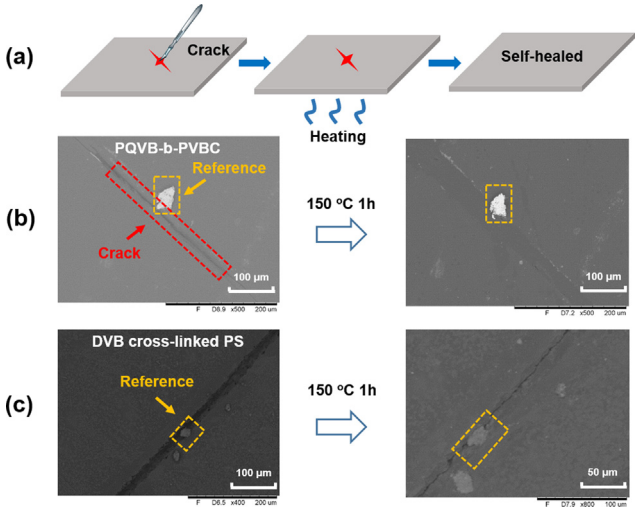

Fig. 6. The Self-healing of PQVB-b-PVBC membrane. (a) Schematics showing the self-healing of membrane samples. (b) The SEM images a cracked PQVB-b-PVBC membrane sample before and after self-healing. The crack is man-made by a sharp knife, as highlighted in the red rectangle. A reference is placed for observation. After heating the membrane sample at 150 °C for 1 h, the crack disappeared. (c) As the control, a DVB cross-linked PS membrane underwent the same procedure, while the surface was not healed after heat treatment. (For interpretation of the references to color in this figure legend, the reader is referred to the web version of this article.)

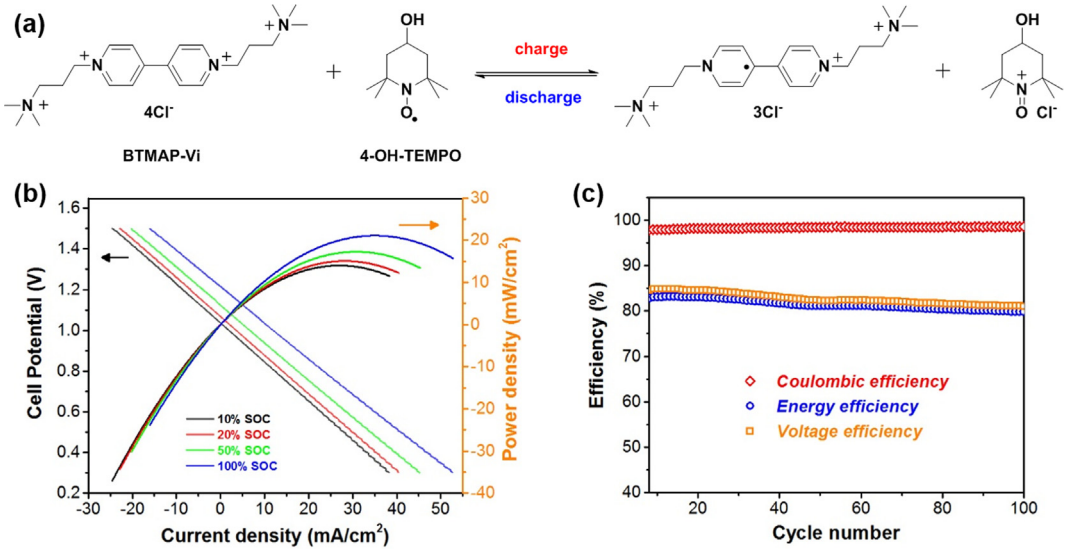

Fig. 7. The Cell performance of a pH 7 4-OH-TEMPO/BTMAP-Vi aqueous organic redox flow battery at room temperature. (a) Structure of the positive and negative electrolytes and the chemical reaction during charge and discharge. (b) Cell polarizations at 10%, 20%, 50% and ~ 100% state of charge (SOC). (c) Coulombic efficiency, energy efficiency and voltage efficiency of the cell during 100 consecutive charge/discharge cycles at 10 mA cm^{-2} with cutoff voltages at 1.6 V for the charge process and 0.5 V for the discharge process. Electrolyte composition: 10 mL of 0.1 M BTMAP-Vi in 1 M NaCl for the negative side and 10 mL of 0.1 M 4-OH-TEMPO in 1 M NaCl for the positive side.

3.5. Mechanical strength

Tensile strength of wet PQVB-b-PVBF membrane samples was measured to evaluate whether the membrane could withstand the mechanical force inside a cell stack of a practical application. The pristine membrane peeled off from petri dish is brittle, with an elongation at break of 1.2% and a yielding stress of 6.7 MPa. It can hardly meet the long term operation requirement of any battery devices and it broke into pieces when we assembled a cell with the pristine membrane. However, when we heated the membrane samples to 150 °C and then slowly cooled them to room temperature, the mechanical strength of wet membrane samples is significantly enhanced, with the elongation at break of 2.7% and the yielding stress of 17.1 MPa. The annealed membrane samples were 3 times stronger than the pristine ones due possibly to the elimination of the internal stress in PQVB-b-PVBF membrane. Therefore, after annealing treatment, the PQVB-b-PVBF membrane can withstand the stress during the cell assembly.

3.6. Cell performance

Considering the superior Cl^- conductivity, moderate water swelling and acceptable mechanical strength, we applied the self-healing PQVB-b-PVBF membrane (with a thickness of 188 μm), in a pH 7 aqueous organic redox flow battery. We here choose a reported negative electrolyte containing bis(3-trimethylammonio)propyl viologen tetrachloride (BTMAP-Vi) and a reported positive electrolyte containing 4-hydroxy-2,2,6,6-tetra methylpiperidin-1-oxyl (4-OH-TEMPO) and the redox pairs can theoretically provide an open circuit voltage of 1.16 V (Beh et al., 2017; Liu et al., 2016), as presented in Fig. 7a. The battery was running at room temperature with a BTMAP-Vi aqueous solution of 0.1 M in 1 M NaCl on the negative side and a 4-OH-TEMPO aqueous solution of 0.1 M in 1 M NaCl on the positive side. These solutions were circulated within a typical redox flow battery device. The polarization curves of the assembled cell were measured at 10, 20, 50 and ~ 100% state of charge (SOC), respectively (Fig. 7b). At ~ 100% SOC, the cell delivered a maximum power density of 21 mW cm^{-2} at a current density of 37 mA cm^{-2}.

The cell was then galvanostatically cycled at a current density of 10 mA cm^{-2} for 100 consecutive cycles (Fig. 7c). Coulombic efficiency of the cell maintains at >97%, indicating the stable charge-discharge without obvious electrolyte crossover. A stable round-trip energy efficiency exceeds 79% and a voltage efficiency is over 80%. The results demonstrate that our membrane could be a promising membrane for pH 7 aqueous organic redox flow battery. Further optimization of battery performance is now ongoing. We attempted to evaluate the cell performances of a membrane sample that self-healed from a man-made crack. However, the mechanical strength of the self-healed AEM sample appears to be poorer than the pristine ones. We believe this is due to the rigid polystyrene chains and replacing polystyrene backbone with flexible ones or attaching flexible side chains to the polymer backbone would be promising strategy to solve the problem. This will be tested in a future work.

4. Conclusions

By exploiting the reversible nature of DA reaction, we devised a self-healing AEM from styrene derivatives by RAFT polymerization. We recorded and confirmed the self-healing of a crack at 150 °C on the PQVB-b-PVBF membrane surface via SEM. The membrane is positively charged and can transport anions, with a Cl^- conductivity of 32.7 mS/cm at 80 °C. Water swelling of PQVB-b-PVBF membrane was also suppressed in the DA reaction cross-linked polymer network. Therefore, it promises a cost-effective and durable AEM for a pH 7 aqueous redox flow battery. As the proof of concept, the battery delivered stable cycling performance over 100 consecutive charge/discharge cycles, with a coulombic efficiency of >97% and an energy efficiency of >79%. This work highlights the possibility to develop a self-healing AEM using DA reaction and its practical application in a demonstrative flow battery. We envision that this could be extended to fuel cells and other batteries. Future efforts will be devoted to exploring more robust AEMs that can self-heal cracks in-situ.

Conflict of interest

None.

Acknowledgements

This project has been supported by the National Natural Science Foundation of China (Nos. 21720102003, 91534203, 21878281, 21506201), International Partnership Program of Chinese Academy of Sciences (No. 21134ky5b20170010), K.C. Wong Education Foundation (2016-11) and Changjiang Scholars Program Funding (2014). The numerical calculations were performed on the supercomputing system in the Supercomputing Center at the University of Science and Technology of China.

Appendix A. Supplementary material

Supplementary data to this article can be found online at https://doi.org/10.1016/j.ces.2019.02.033.

References

Amel, A., Gavish, N., Zhu, L., Dekel, D.R., Hickner, M.A., Ein-Eli, Y., 2016. Bicarbonate and chloride anion transport in anion exchange membranes. J. Membr. Sci. 514, 125–134.

An, Q., Qian, J., Yu, L., Luo, Y., Liu, X., 2005. Study on kinetics of controlled/living radical polymerization of acrylonitrile by RAFT technique. J. Polym. Sci., Part A: Polym. Chem. 43, 1973–1977.

Beh, E.S., De Porcellinis, D., Gracia, R.L., Xia, K.T., Gordon, R.G., Aziz, M.J., 2017. A neutral pH aqueous organic-organometallic redox flow battery with extremely high capacity retention. ACS Energy Lett. 2, 639–644.

Cao, Y., Morrissey, T.G., Acome, E., Allec, S.I., Wong, B.M., Keplinger, C., Wang, C., 2017. A transparent, highly stretchable self-healing, ionic conductor. Adv. Mater. 29.

Chen, X., Dam, M.A., Ono, K., Mal, A., Shen, H., Nutt, S.R., Sheran, K., Wudl, F., 2002. A Thermally re-mendable cross-linked polymeric material. Science 295, 1698.

Fuhrmann, A., Gostl, R., Wendt, R., Kotteritzsch, J., Hager, M.D., Schubert, U.S., Brademann-Jock, K., Thunemann, A.F., Nochel, U., Behl, M., Hecht, S., 2016. Conditional repair by locally switching the thermal healing capability of dynamic covalent polymers with light. Nat. Commun. 7, 13623.

Haas, H.C., MacDonald, R.L., 1973. Maleimide polymers. I. A polymeric color reaction. J. Polym. Sci.: Polym. Chem. Ed. 11, 327–343.

He, Y., Wu, L., Pan, J., Zhu, Y., Ge, X., Yang, Z., Ran, J., Xu, T., 2016. A mechanically robust anion exchange membrane with high hydroxide conductivity. J. Membr. Sci. 504, 47–54.

Hou, J., Liu, Y., Ge, Q., Yang, Z., Wu, L., Xu, T., 2018. Recyclable cross-linked anion exchange membrane for alkaline fuel cell application. J. Power Sources 375, 404–411.

Jo, Y.Y., Lee, A.S., Baek, K.-Y., Lee, H., Hwang, S.S., 2017. Thermally reversible self-healing polysilsesquioxane structure-property relationships based on Diels-Alder chemistry. Polymer 108, 58–65.

Kavitha, A.A., Singha, N.K., 2009. "Click Chemistry" in Tailor-made polymethacrylates bearing reactive furfuryl functionality: a new class of self-healing polymeric material. ACS Appl. Mater. Interfaces 1, 1427–1436.

Kuhl, N., Hopkinson, M.N., Glorius, F., 2012. Selective rhodium(III)-catalyzed cross-dehydrogenative coupling of furan and thiophene derivatives. Angew. Chem., Int. Ed. Engl. 51, 8230–8234.

Kwasny, M.T., Zhu, L., Hickner, M.A., Tew, G.N., 2018. Thermodynamics of Counterion release is critical for anion exchange membrane conductivity. J. Am. Chem. Soc. 140, 7961–7969.

Lai, J.C., Mei, J.F., Jia, X.Y., Li, C.H., You, X.Z., Bao, Z., 2016. A stiff and healable polymer based on dynamic-covalent boroxine bonds. Adv. Mater. 28, 8277–8282.

Li, H., Bai, J., Shi, Z., Yin, J., 2016. Environmental friendly polymers based on schiff-base reaction with self-healing, remolding and degradable ability. Polymer 85, 106–113.

Li, Y., Liang, L., Liu, C., Li, Y., Xing, W., Sun, J., 2018. Self-healing proton-exchange membranes composed of nafion-poly(vinyl alcohol) complexes for durable direct methanol fuel cells. Adv. Mater. 30, e1707146.

Lin, C.X., Zhuo, Y.Z., Hu, E.N., Zhang, Q.G., Zhu, A.M., Liu, Q.L., 2017. Crosslinked side-chain-type anion exchange membranes with enhanced conductivity and dimensional stability. J. Membr. Sci. 539, 24–33.

Liu, T., Wei, X., Nie, Z., Sprenkle, V., Wang, W., 2016. A total organic aqueous redox flow battery employing a low cost and sustainable methyl viologen anolyte and 4-HO-TEMPO catholyte. Adv. Energy Mater. 6, 1501449.

Mehmood, A., Scibioh, M.A., Prabhuram, J., An, M.-G., Ha, H.Y., 2015. A review on durability issues and restoration techniques in long-term operations of direct methanol fuel cells. J. Power Sources 297, 224–241.

Röttger, M., Domenech, T., van der Weegen, R., Breuillac, A., Nicolaÿ, R., Leibler, L., 2017. High-performance vitrimers from commodity thermoplastics through dioxaborolane metathesis. Science 356, 62.

Ran, J., Wu, L., He, Y., Yang, Z., Wang, Y., Jiang, C., Ge, L., Bakangura, E., Xu, T., 2017. Ion exchange membranes: new developments and applications. J. Membr. Sci. 522, 267–291.

Sata, T., Yamaguchi, T., Matsusaki, K., 1995. Effect of hydrophobicity of ion exchange groups of anion exchange membranes on permselectivity between two anions. J. Phys. Chem. 99, 12875–12882.

Sumerlin, B.S., 2018. Next-generation self-healing materials. Science 362, 150.

Tang, S.K.Y., Marshall, W.F., 2017. Self-repairing cells: How single cells heal membrane ruptures and restore lost structures. Science 356, 1022.

Taylor, D.L., In Het Panhuis, M., 2016. Self-healing hydrogels. Adv. Mater., vol. 28, pp. 9060–9093.

Tee, B.C.K., Wang, C., Allen, R., Bao, Z., 2012. An electrically and mechanically self-healing composite with pressure- and flexion-sensitive properties for electronic skin applications. Nat. Nanotechnol. 7, 825.

Trovatti, E., Lacerda, T.M., Carvalho, A.J., Gandini, A., 2015. Recycling tires? Reversible crosslinking of poly(butadiene). Adv. Mater. 27, 2242–2245.

Wang, L., Hickner, M.A., 2014. Low-temperature crosslinking of anion exchange membranes. Polym. Chem. 5, 2928.

Wang, Y., Huang, F., Chen, X., Wang, X.-W., Zhang, W.-B., Peng, J., Li, J., Zhai, M., 2018. Stretchable, conductive, and self-healing hydrogel with super metal adhesion. Chem. Mater. 30, 4289–4297.

Wu, J., Cai, L.H., Weitz, D.A., 2017. Tough self-healing elastomers by molecular enforced integration of covalent and reversible networks. Adv. Mater. 29.

Yang, Z., Hou, J., Wang, X., Wu, L., Xu, T., 2015. Highly water resistant anion exchange membrane for fuel cells. Macromol. Rapid Commun. 36, 1362–1367.

Zhang, G., Zhao, Q., Yang, L., Zou, W., Xi, X., Xie, T., 2016. Exploring dynamic equilibrium of Diels-Alder reaction for solid state plasticity in remoldable shape memory polymer network. ACS Macro Lett. 5, 805–808.

Zhang, H.W., Chen, D.Z., Xianze, Y., Yin, S.B., 2015. Anion-exchange membranes for fuel cells: synthesis strategies, properties and perspectives. Fuel Cells 15, 761–780.

Zhu, L., Zimudzi, T.J., Li, N., Pan, J., Lin, B., Hickner, M.A., 2016. Crosslinking of comb-shaped polymer anion exchange membranes via thiol–ene click chemistry. Polym. Chem. 7, 2464–2475.